On the emergence of an Arctic amplification signal in terrestrial Arctic snow extent

Debjani Ghatak,[1] Allan Frei,[2] Gavin Gong,[3] Julienne Stroeve,[4] and David Robinson[5]

Received 4 February 2010; revised 1 September 2010; accepted 1 October 2010; published 18 December 2010.

[1] The impact of declining sea ice in amplifying surface air temperatures (SAT) over the Arctic Ocean is readily visible, and this "Arctic amplification" will become more pronounced as more sea ice is lost in the coming decades. The effect of sea ice loss on atmospheric temperatures and circulation patterns is of utmost significance as these changes will affect the terrestrial climate. Land-surface snow is vulnerable to these changes; hence, we search for any link between changes in Arctic sea ice and Northern Hemisphere snow cover. Analyses of observational data sets suggest that the increasing snow cover over Siberia during fall and early winter is correlated with the decreasing September Arctic sea ice over the Pacific sector. We also examine modeled covariance between sea ice and snow using historical and future simulations of the Community Climate System Model (CCSM3). Results indicate the emergence of a Siberian snow signal during the last half of the 21st century most strongly during late winter. Moreover, CCSM3 future simulations show diminishment of snow at a hemispheric scale outside of the Siberian region, which is correlated with the loss of Arctic sea ice. These results indicate that we may be seeing the first, albeit weak, signs of "Arctic amplification" on the terrestrial Arctic snowpack; that only a weak and therefore inconclusive signal would be expected at this time; and that the signal should strengthen over the coming decades.

Citation: Ghatak, D., A. Frei, G. Gong, J. Stroeve, and D. Robinson (2010), On the emergence of an Arctic amplification signal in terrestrial Arctic snow extent, *J. Geophys. Res.*, *115*, D24105, doi:10.1029/2010JD014007.

1. Introduction

[2] The status of the rapidly declining Arctic sea ice has been closely monitored for more than a decade now [e.g., *Cavalieri et al.*, 1997; *Rothrock et al.*, 1999; *Parkinson et al.*, 1999; *Stroeve et al.*, 2005, 2007; *Serreze et al.*, 2007; *Comiso et al.*, 2008]. Considering the crucial role of sea ice in the climate system, many researchers have investigated the effects of retreating sea ice on present and projected future atmospheric temperatures and circulation patterns [e.g., *Honda et al.*, 1999; *Deser et al.*, 2000; *Magnusdottir et al.*, 2004; *Alexander et al.*, 2004; *Kvamstø et al.*, 2004; *Gerdes*, 2006; *Singarayer et al.*, 2006; *Francis et al.*, 2009; *Deser et al.*, 2010]. One of the major impacts is already apparent in the amplification of rising surface air temperatures (SAT) over the Arctic ocean, as suggested by the concept of "Arctic amplification" [*Serreze et al.*, 2009]. Expanding open water areas in summer allows for heating of the ocean's mixed layer and therefore a net heat gain by the ice-ocean column during summer; this subsequently leads to a delayed autumn freeze-up. The insulating effect of sea ice during autumn is then weakened due to the thinner and the smaller ice pack, which results in a large heat loss from the ocean to the atmosphere which further amplifies the atmospheric warming [*Serreze and Francis*, 2006; *Serreze et al.*, 2009]. Moreover, it is expected that amplified warming from the loss of the summer sea ice cover will spread over high-latitude land areas, hastening degradation of permafrost [*Lawrence et al.*, 2008].

[3] Model simulations indicate increased SAT over high latitudes and shifts in precipitation patterns and amounts in response to a prescribed future reduction in Arctic sea ice [*Singarayer et al.*, 2006; *Deser et al.*, 2010]. *Francis et al.* [2009] also examined changes in winter precipitation due to historical summer sea ice variability through the analysis of observational and reanalysis data sets, and suggest negative anomalies in precipitation over the Northeast Atlantic extending into northern Europe and also over much of U.S. and Alaska.

[4] It is reasonable to hypothesize that these changing atmospheric and terrestrial climates may play a significant role in affecting the snow over the surrounding landmasses. The impact of increased SATs on snow cover depends on whether the change in temperature crosses the freezing point. Over regions where temperatures do cross the freezing point,

[1]Program in Earth and Environmental Sciences, CUNY Graduate Center, City University of New York, New York, New York, USA.
[2]Department of Geography, Hunter College, Program in Earth and Environmental Sciences, City University of New York, New York, New York, USA.
[3]Department of Earth and Environmental Engineering, Columbia University, New York, New York, USA.
[4]National Snow and Ice Data Center, Cooperative Institute for Research in Environmental Sciences, University of Colorado, Boulder, Colorado, USA.
[5]Department of Geography, Rutgers University, Piscataway, New Jersey, USA.

0148-0227/10/2010JD014007

snowfall is partially or wholly replaced by rain, and snowmelt is increased, resulting in a diminished snowpack. Over regions that remain below freezing after the warming, snowfall and snow cover are typically enhanced because of the increased moisture capacity of the atmosphere.

[5] *Barry et al.* [2007] reported that ECHAM5 model simulations for 21st century climate show a decrease of 60% to 80% in monthly maximum SWE over most of the mid-latitudinal region of the Northern Hemisphere between 1981 and 2000 and 2080–2100, but an increase over the Canadian Arctic and Siberia. *Deser et al.* [2010] (from now on DTAL10) specifically examined projected future changes in snow over the Northern Hemisphere as a result of retreating Arctic sea ice using the Community Atmosphere Model version 3 (CAM3). They identified an increase in snow depth (SND) over Siberia in response to the prescribed future loss of sea ice concentration and thickness.

[6] While the aforementioned modeling experiments describe expected changes in snow due to declining sea ice in the future, we focus on whether there is currently any observational evidence of an emerging climate change signal, and/or sea ice related signal in Northern Hemisphere snow cover changes. Specifically, we investigate the observed covariance between early season snow and the preceding summer sea ice, and the modeled covariance between these two fields for both recent and future time periods. We focus on fall and early winter season snow to represent the snowpack accumulation period, and the preceding September sea ice which is the month of climatological minimum sea ice cover. Since, the impact of "Arctic amplification" is readily visible over the high-latitude region during the autumn season [*Serreze et al.*, 2009], it is prudent to examine the land-surface snow during this season for any emerging signal of links between declining sea ice cover and snow cover. We also discuss possible physical mechanisms linking sea ice changes to snow cover.

2. Data Sets, Model Outputs, and Methodology

2.1. Data Sets and Model Outputs

[7] The spatial domain of our study spans the extra-tropical Northern Hemisphere. EASE-grid (Equal Area Scalable Earth Grid) snow extent data [*Armstrong and Brodzik*, 2005] based on NOAA-NESDIS snow charts, and sea ice concentration [*Comiso*, 1999] data from Scanning Multichannel Microwave Radiometer (SMMR) and Special Sensor Microwave/Imager (SSM/I) sensors, have been obtained from the National Snow and Ice Data Center (NSIDC). The use of weekly snow information provides the opportunity to compute an annual time series of the total number of weeks of autumn and early winter (defined here as October through December, OND) snow cover (SNE) for the period 1979–2007 at each grid point. The mean September sea ice field is also generated for the same 29 year time period from the sea ice concentration (SIC) data set which has been produced using a Bootstrap algorithm. No data above 83° N is included during the processing of SIC data. Both SNE and SIC data sets are available at a spatial resolution of 25 km; but are regridded to 100 km resolution for our hemispheric-scale analysis. We also use a mean September Arctic sea ice extent time series available from NSIDC's Sea Ice Index (http://nsidc.org/data/seaice_index).

[8] We use archived output from the Intergovermental Panel on Climate Change fourth assessment report (IPCC AR4), produced by the Community Climate System Model version 3 (CCSM3), a fully coupled atmosphere-ocean general circulation model (AOGCM). Arctic sea ice variability is simulated well by this model [*Holland et al.*, 2006; *Stroeve et al.*, 2007]. Historical simulations as well as 21st century simulations from the SRESA1B scenario (Special Report on Emissions Scenarios; gradual rise to 720 ppm of atmospheric CO_2 concentrations by 2100) are utilized for this study. Model outputs for three variables, "surface snow area fraction where land" (SNC in %, as named by IPCC), "surface snow thickness" (SND in meter, as named by IPCC) and "sea ice area fraction" (SIC in %, as named by IPCC) are used here (http://www-pcmdi.llnl.gov/ipcc/standard_output.html#Experiments). For both the observational data and for the model output, grid cells with less than 15% sea ice concentration have been excluded in the analysis, because 15% SIC isopleth is considered as the cutoff for ice extent [*Stroeve et al.*, 2007]. We use the ensemble mean of three runs (Runs 1, 5, and 6), which are the only ensemble members available for all fields at the time of the preparation of this manuscript.

2.2. Methodology

[9] Singular Value Decomposition Analysis (SVD) is applied here to snow and sea ice fields, where each field consists of a 29 year long time series at each grid point. SVD is a useful method to extract coupled patterns from two space-time fields and has been used in many studies [*Prohaska*, 1976; *Lanzante*, 1984; *Wallace et al.*, 1992; *Cherry*, 1997; *Rajagopalan et al.*, 2000; *Stroeve et al.*, 2008]. Here, we employ the correlation matrix approach as these two fields have different units of measurements. SVD analysis produces pairs of spatial patterns, explaining maximum mean squared temporal covariance between two space-time fields. It also generates pairs of temporal coefficient (TC) time series describing the temporal evolutions of their corresponding spatial patterns [*Bretherton et al.*, 1992]. Negative TC time series values indicate that the pattern of variability follows the SVD result but with the signs reversed. We present the SVD results as heterogeneous correlation (HC) maps rather than SVD mode maps, where the HC map is computed by correlating the time series at each grid point of one field with the corresponding TC of the other field. Here, we employ non-parametric Spearman correlation coefficients (ρ) to compute HC maps and report only results which exceed 95% confidence level. We also discuss results of composite analysis.

3. Results

3.1. Observational Results

[10] Figure 1 presents the leading mode of the SVD analysis between mean September SIC and OND SNE, which explains 31% of the covariance between the two fields. The regions of significant correlation between the SIC and SNE fields are the Pacific sector of the Arctic Ocean and northern Asia, respectively. The SNE pattern (Figure 1a) is strongest ($|\rho| > 0.7$) over the Siberia region. The SIC pattern (Figure 1b) is strongest ($|\rho| > 0.7$) over the Beaufort and Chukchi seas. Correlation pattern values for the two fields are of opposite sign, indicating an inverse relationship between SNE and SIC. The TC time series

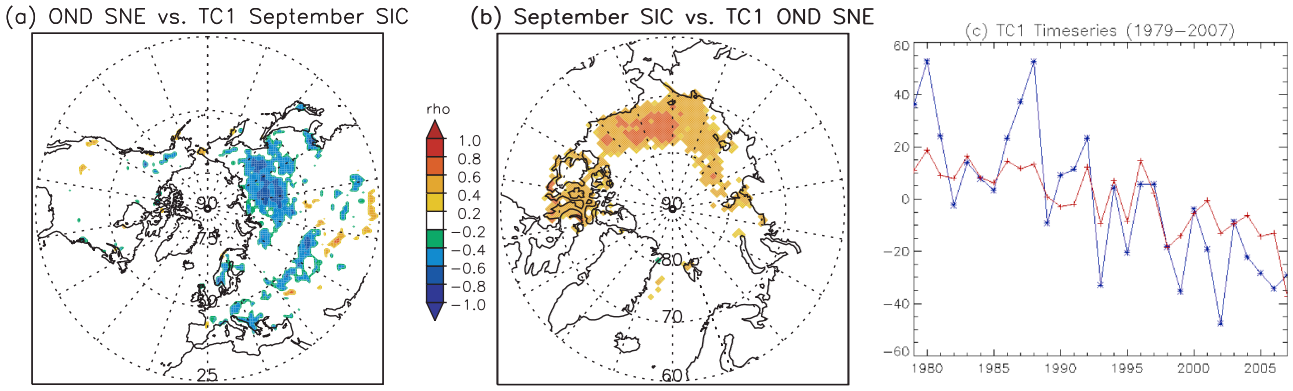

Figure 1. The first SVD mode between OND SNE and September SIC for the 1979–2007 time period. Heterogeneous correlation maps: (a) OND SNE versus TC1 September SIC and (b) September SIC versus TC1 OND SNE; (c) TC1 time series from both fields (red = SIC, blue = SNE). Units in the *y* axis are arbitrary; therefore they are not shown.

(Figure 1c) for both fields are positively correlated with each other (r = 0.81), indicating significant covariability. Moreover, the two TC time series exhibit an overall negative trend from positive to negative values over the study period of 1979–2007. These results indicate that the strongest covariability signal between these two fields is associated with gradually increasing snow over Siberia and declining sea ice over the Arctic Ocean.

[11] SVD analysis between these two variables was repeated after detrending the parameter fields (results not shown here). Using ordinary least square regression, we remove the trend from the time series at each grid point for both of the original space-time fields of SNE and SIC, and then use these fields for SVD analysis. The HC maps generated from the leading mode show no significant correlations between Siberian SNE and Arctic SIC. Thus, this set of analysis suggests that the primary pattern of correlation between two fields identified in Figure 1 is driven mainly by the trends in both fields. This does not imply any cause and effect relationship. However, because the trend is so strong, and recent sea ice coverage in the Pacific sector of the Arctic is so far below earlier values, the possibility remains that there is an influence of recent dramatically low sea ice years on Siberian snow, but that earlier "low" years were not low enough to impact the snow cover.

[12] To evaluate the relationship further, we compute the differences in OND SNE between two 9 year composites, which consist of the nine extreme low and nine extreme high mean September sea ice extent years from the period of 1979–2007. Nine extreme high years are 1996, 1980, 1992, 1986, 1983, 1988, 1987, 1982, and 1981 and nine extreme low years are 2007, 2005, 2006, 2002, 2004, 1995, 2003, 1990, and 1999. This composite analysis was performed both with and without detrending the sea ice extent time series. Figure 2 presents the results for the (low SIC – high SIC) difference, i.e., the SNE response to decreasing SIC. We only show the composite difference at grid points where each of the two 9 year composites has significantly different means at significance level of 0.05 following student's *t* statistic. When the original time series is used, the composite difference (Figure 2a) indicates extended OND SNE over Siberia (as well as at scattered grid points in other regions) following low summer sea ice extent. In the composite difference map using the detrended sea ice extent time series (Figure 2b) the Siberian signal is mostly eliminated.

[13] These sets of composite analyses confirm the results from SVD analyses that the interannual trends in both fields drive the relationship between Siberian snow and the Arctic sea ice. Thus, it indicates an emerging signal of climate change as opposed to a signature of interannual climate variability. Composite analyses based on 5 year composites produce similar conclusions.

3.2. Results Based on Modeling Output

[14] We also performed SVD analyses on mean OND SNC and mean September SIC using CCSM3 historical and 21st century simulations. Here, the analysis is repeated using four time domains (1979–2007, 1979–2020, 1979–2050 and 1979–2080), to reveal how the leading pattern of covariability between snow and sea ice changes as the time domain extends farther into the future. Figure 3 presents the resulting HC maps and TC time series for all four time domains. The TC time series are significantly and positively correlated with each other during each time domain (R values = 0.95, 0.95, 0.97 and 0.97, respectively, for four time domains).

[15] As one scans the four SNC patterns (Figures 3a–3d), a broad region of positive correlation emerges and grows throughout the 21st century. During the 1979–2007 time domain, isolated SNC patterns (Figure 3a) occur mainly over Scandinavia and over midlatitudinal areas of North America. This pattern gradually spreads over NW Europe and over the interior of North America during the 1979–2020 time period (Figure 3b). By the end of the century, most of the Northern Hemisphere is affected (Figures 3c and 3d), except for eastern Siberia.

[16] During 1979–2007, the HC SIC pattern exhibits strongest positive correlations over the Atlantic sector of the Arctic (Figure 3e). This spatial pattern is different than what has actually been observed in recent years where major ice loss has primarily occurred in the Pacific sector [*Stroeve et al.*, 2005; *Serreze et al.*, 2007] (see Discussion). Between 2007 and 2080 the SIC pattern spreads strongly over the Pacific sector (Figures 3f, 3g, and 3h). The TC time series

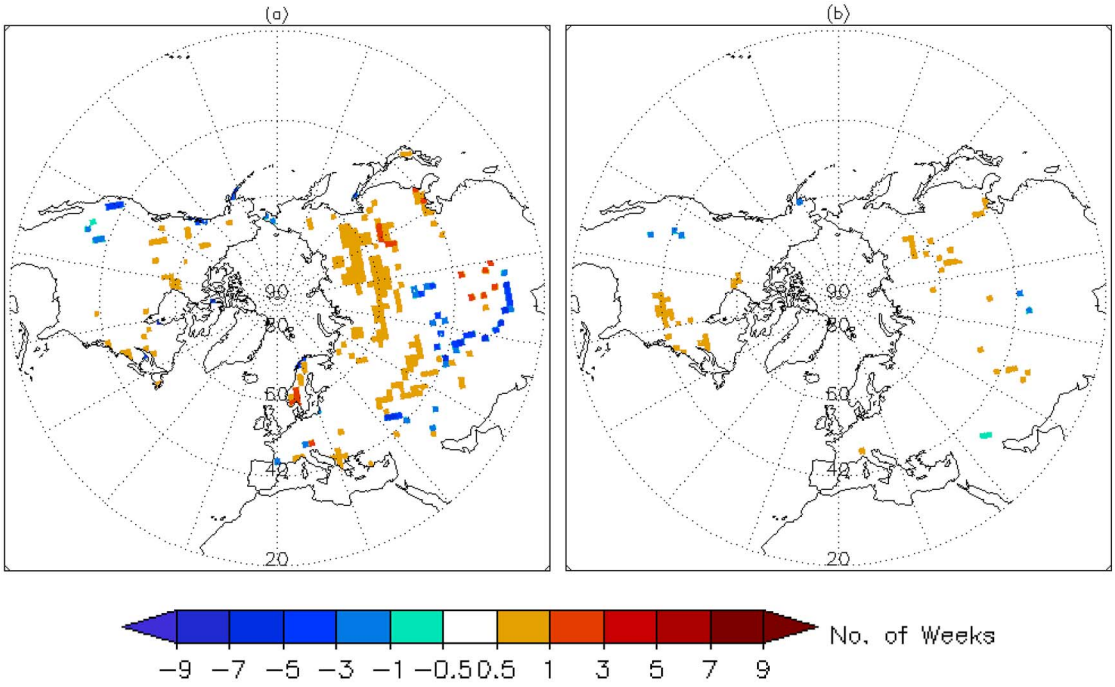

Figure 2. Difference in total number of weeks of snow cover during OND between two 9 year Composites of low versus high September sea ice extent years; (a) composites based on actual time series; (b) composites based on detrended time series.

show negative trends during all time domains (Figures 3i–3l), although in the 1979–2080 analysis (Figure 3l) the time series flattens out in later years as a result of the virtually complete disappearance of sea ice by midcentury.

[17] Similar analysis has been done between mean OND SND and mean September SIC for the same four time domains because this snow metric provides information not only about the presence or absence of snow but also regarding the volume of snow. Unfortunately, observations of long-term and reliable hemispheric-scale snow depth data are not available, and therefore only SNE was used in the observational analysis. The modeled HC SIC pattern and the TC time series from the leading mode of this SVD analysis are virtually indistinguishable with the patterns presented in Figures 3e–3l. Therefore, we only present the HC SND pattern in Figures 3m–3p. These four Figures (3m–3p) of SND are also very similar with the Figures 3a–3d where SNC has been used; the only difference is that the correlated region over Siberia appears more spatially extensive in the Figures (3o and 3p) using SND. Correlation coefficients are reversed in sign from the rest of the hemisphere over Siberia. This reversed Siberian pattern is undetectable during 1979–2007 time domain, but it emerges by midcentury.

[18] This series of SVD analyses show a gradual spreading of a climate change impact on snow across Northern Hemisphere lands during the 21st century. The signal consists of a hemisphere-wide diminishment of snow except over Siberia where an increase in snow depth emerges around midcentury, and this snow pattern is correlated with the decreasing sea ice over the Arctic.

[19] In order to confirm that our results are not an artifact of increasing the number of points (n) in each successive SVD, we performed the SVD analyses between mean OND SNC and mean September SIC for four time domains that have the same number of years (n = 29). The time domains are 1979–2007, 1992–2020, 2022–2050 and 2052–2080 (results not shown here). The results are consistent with those presented in Figure 3. The correlations strengthen in each successive time period up to, and including, the third one (2022–2052). During the 2052–2080 time period, the sea ice has already disappeared, and therefore the correlation disappears as well.

[20] We repeated SVD analysis for the identical four time domains using modeled mean winter (JFM) instead of fall (OND) SNC. As these SVD analyses have been done between modeled JFM SNC and the preceding September SIC, the time domain is marked as 1980–2008 in Figure 4a and likewise for the corresponding time periods in Figures 4b–4d; though the four time domains in Figure 4 are essentially same as the previous analyses. Figure 4 presents only the resulting SNC pattern, because the SIC pattern is similar to the previous SVD analysis (Figures 3e–3h). The correlated region of JFM SNC is more spatially extensive and coherent than during OND (compare Figures 4a–4d to Figures 3a–3d). Of particular interest is that the pattern over Siberia is more spatially extensive and has higher correlations. This result holds true when we repeat this analysis involving JFM SND. This is consistent with DTAL10 in which a stronger SND signal was reported over Siberia during late winter as opposed to fall/early winter.

[21] It is interesting to note that the observation-based SVD indicates a climate change signal is already emerging in snow cover, while the model-based SVD does not reveal such a signal until the mid-21st century. It is possible that

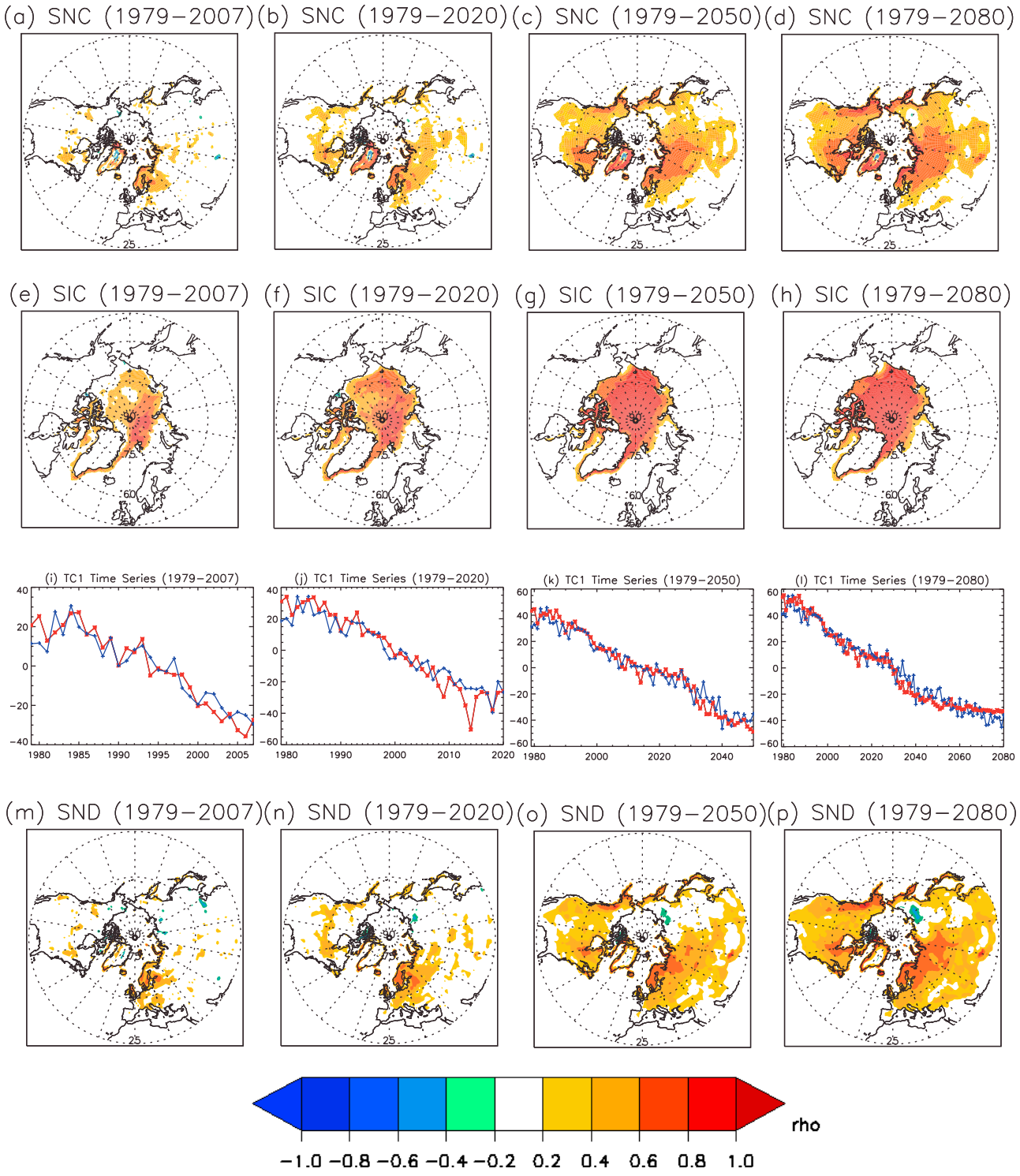

Figure 3. Leading SVD mode between OND SNC and September SIC for different time domains derived from the CCSM3 model. Heterogeneous correlation maps (a)–(d) OND SNC versus TC1 September SIC and (e–h) September SIC versus TC1 OND SNC; (i–l) TC1 time series from both fields (red = SIC, blue = SNC). Similar analysis has been done between OND SND and September SIC, only shown here heterogeneous correlation maps from the leading mode for (m–p) OND SND versus TC1 September SIC.

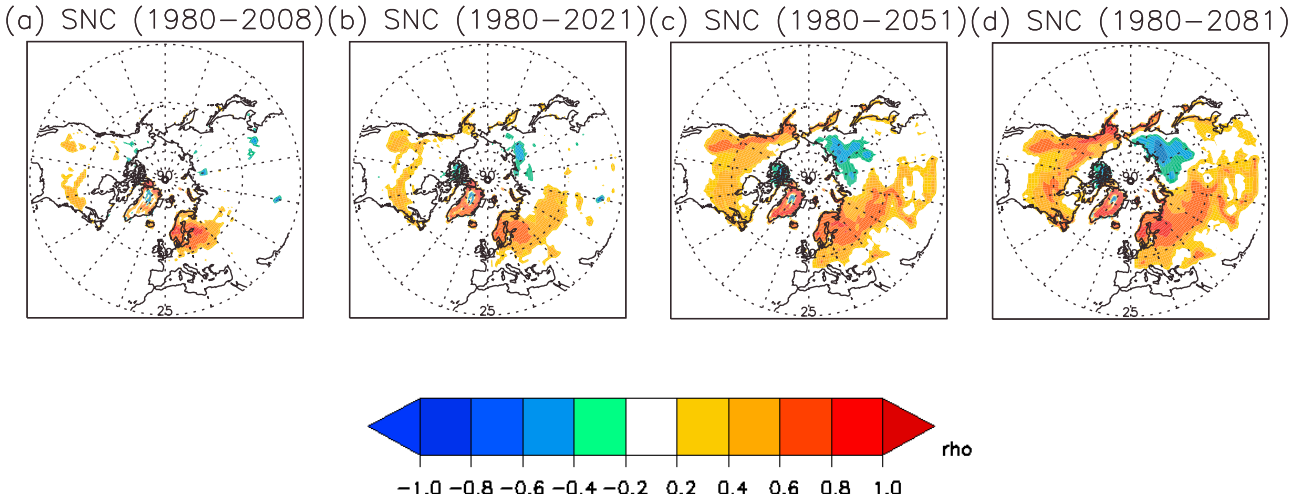

Figure 4. Heterogeneous correlation maps of the leading SVD mode between JFM SNC and September SIC for different time domains derived from the CCSM3 model; only shown here (a–d) JFM SNC versus TC1 September SIC.

climate models lag the actual climate system in the timing of this effect, if for no reason other than their sea ice predictions, which have been shown to lag behind observed sea ice reductions [*Stroeve et al.*, 2007]. In addition, the signal in the SIC pattern based on CCSM3 model outputs is mainly over the Atlantic sector of the Arctic Ocean during the early 21st century, whereas recent sea ice losses have actually occurred mainly over the Pacific sector. Since the model has yet to capture the precursive regional sea ice loss in the early 21st century, it is not surprising that it does not capture the consequent early 21st century Siberian snow signal.

4. Discussion

[22] We demonstrate empirically, using SVD analysis, that the primary signal of covariability between Arctic sea ice and Northern Hemisphere SNE between 1979 and 2007 consists of a decreasing trend in September SIC primarily over the Pacific sector, which is correlated to an increasing trend in fall and early winter SNE over Siberia. Composite analyses corroborate that SNE over Siberia has increased following the low summer sea ice during this time period. These relationships do not alone imply any cause and effect relationship.

[23] These results are consistent with the spatial patterns as suggested by *Bulygina et al.* [2009], which shows the increase in the duration of snow cover over central Siberia (Yakutia) and Far East. Another study of the Lena River Basin shows a positive trend in monthly precipitation during winter months, specifically in November and December [*Yang et al.*, 2002]. They indicated that more winter precipitation likely results in greater snow cover and snowpack storage, and leads to the increased snowmelt runoff and streamflow during early summer.

[24] Next we compare the empirical results with results from analogous SVD analyses between sea ice and snow from CCSM3 20th to 21st century climate simulations. We analyze model results for four different temporal domains: 1979–2007 (which coincides with our empirical analysis), 1979–2020, 1979–2050, and 1979–2080. Climate model comparisons show weaker correlations between September sea ice loss and snow over Siberia during OND (i.e., increase in snow), but the correlation becomes stronger during JFM. This signal is most prominent during the last half of the century. In addition, the model-based SVD indicates a diminished snow across all Northern Hemisphere lands outside of Siberia during both OND and JFM, which is readily visible at hemispheric scales even during the first half of the 21st century. This snow pattern is also correlated with the decreasing sea ice over the Arctic.

[25] While covariance between sea ice and snow cover does not provide a cause and effect, our empirical results may be a first sign of an emerging climate change signal in high-latitude snow cover. One would expect the spatial pattern of changing snow in response to a generalized warming to be similar to the climate model results: i.e., loss of snow over most regions. Existing literatures also indicates declining snow due to rising temperature. A study by *Ye et al.* [2003] suggested earlier snowmelt and streamflow changes due to regional climate warming over southern parts of Siberia. Another paper by *Ye et al.* [2008] indicates that rain-on-snow days increased over European Russia and increased air temperature is the primary attributing factor. Moreover, the ACIA report showed that Arctic warming caused 10% loss of snow cover extent over the last 30 years [*Hassol*, 2004]. *Räisänen* [2008] also examined changes in the projected 21st century snow water equivalent (SWE) in response to the greenhouse gas warming through the analysis of 20 global climate models output participating in the 3rd Coupled Model Intercomparison Project (CMIP3). He found SWE decreasing during winter over terrestrial regions in Northern Hemisphere, except over northernmost North America and Siberia where SWE increases, and identified −20°C isotherm in late 20th century winter (NDJFM) mean temperature as the threshold temperature for the SWE changes.

[26] But even under a warming scenario, some areas still may exist that are sufficiently cold to maintain a snow cover. Furthermore, over such colder regions, a warmer (but still below freezing) atmosphere would have a higher capacity

for holding water vapor, and therefore could potentially deliver more snowfall. Thus, an empirical result as shown in this paper, showing the beginning of such a signal over Siberia would be consistent with the expectations, even if the hemisphere-wide signal of diminished snow is not yet found in our results.

[27] Another question is whether the Siberian response identified here represents a manifestation of the terrestrial "Arctic amplification" signal. *Serreze and Francis* [2006] and *Serreze et al.* [2009] discuss the emergence of an Arctic amplification signal over the ocean. The primary source of Arctic amplification is the additional energy introduced into the surface climate system within the Arctic Ocean basin by diminished sea ice (see section 1). The question then is whether this energy input is transported into Siberia to influence snow cover.

[28] There is modeling evidence to support this idea. DTAL10 performed two sets of Community Atmosphere Model version 3 (CAM3) experiments designed to isolate the atmospheric and terrestrial response to depleted Arctic sea ice. Their control experiment includes a repeating seasonal cycle of sea ice (concentrations and thickness) for the period 1980–1999; their perturbation experiment consists of a repeating seasonal cycle of sea ice specified from model results for a period of greatly diminished sea ice, 2080–2099. Same repeating seasonal cycle of SSTs for the period 1980–1999 was specified in both experiments, and GHG concentrations are also fixed at 1980–1999 levels in both experiments. An increase in SND over the Siberian region in response to the prescribed future loss of sea ice concentration and thickness is apparent beginning in November and reaching its maximum in March–April; thus, it is consistent with our observational results for fall and early winter SNE.

[29] Furthermore, DTAL10 and *Finnis et al.* [2007] suggest some links between retreating Arctic sea ice and the terrestrial snow. DTAL10 suggests that the SND increase is a consequence of increased precipitation resulting from diminished sea ice. *Finnis et al.* [2007] show a shift in cyclone-associated precipitation which is a major source of autumn and winter precipitation in midlatitude and high-latitude Northern Hemisphere lands. According to this study, high-latitude regions experience increased precipitation from storms during autumn due to the availability of atmospheric moisture associated with rising temperatures. Moreover, they suggest the role of decreasing sea ice behind this thermodynamic effect on precipitation. *Simmonds and Keay* [2009] also indicates the significant role played by cyclone over the Arctic basin in recent years. *Honda et al.* [2009] also show some mechanisms which may generate some pathways linking sea ice and snow. They show that decreasing summer sea ice thermally generates stationary Rossby waves, which strengthens the Siberian high and causes cold conditions over Eurasia. Further identification of the specific pathways linking sea ice and snow is currently under investigation.

[30] An unfortunate aspect of this problem is that high-latitude climatological observations are extremely limited, and have diminished in numbers in recent years. This is due to budgetary constraints in different countries as well as to the increasing dependence on remotely sensed observations, which cannot provide as much detail on snow cover [*Brown and Armstrong*, 2008]. Thus, while in this paper we point out that there is evidence consistent with the emergence of a sea ice related Arctic amplification signal in the snow cover record, it is too soon to tell. This insufficient observational capacity of high-latitude snow cover may result in the loss of a valuable early indicator of climate change.

[31] **Acknowledgments.** This work has been supported by the NASA Cryospheric Sciences Division (NNX08AQ70G). We thank Mary Jo Brodzik from NSIDC for helping us in acquiring updated data sets and Clara Deser for her insightful comments and suggestions. We are also thankful to the anonymous reviewers for their constructive comments.

References

Alexander, M. A., U. S. Bhatt, J. E. Walsh, M. S. Timlin, J. S. Miller, and J. D. Scott (2004), The atmospheric response to realistic Arctic sea ice anomalies in an AGCM during winter, *J. Clim.*, *17*, 890–905, doi:10.1175/1520-0442(2004)017<0890:TARTRA>2.0.CO;2.

Armstrong, R. L., and M. J. Brodzik (2005), Northern Hemisphere EASE-Grid weekly snow cover and sea ice extent, Version 3, 3 October 1966 to 23 October 1978, Natl. Snow and Ice Data Cent., Boulder, Colo. (Available at http://nsidc.org/data/nsidc-0046.html)

Barry, R. G., R. Armstrong, T. Callaghan, J. Cherry, S. Gearhead, A. Nolin, D. Russell, and C. Zockler (2007), Snow, in *Global Outlook for Ice and Snow*, pp. 39–62, U. N. Environ. Programme, Nairobi.

Bretherton, C. S., C. Smith, and J. M. Wallace (1992), An intercomparison of methods for finding coupled patterns in climate data, *J. Clim.*, *5*, 541–560, doi:10.1175/1520-0442(1992)005<0541:AIOMFF>2.0.CO;2.

Brown, R., and R. L. Armstrong (2008), Snow-cover data: Measurement, products, and sources, in *Snow and Climate: Physical Processes, Surface Energy Exchange and Modeling*, edited by R. L. Armstrong and E. Brun, pp. 181–216, Cambridge Univ. Press, Cambridge, U.K.

Bulygina, O. N., V. N. Razuvaev, and N. N. Korshunova (2009), Changes in snow cover over northern Eurasia in the last few decades, *Environ. Res. Lett.*, *4*, 045026, doi:10.1088/1748-9326/4/4/045026.

Cavalieri, D. J., P. Gloersen, C. L. Parkinson, J. C. Comiso, and H. J. Zwally (1997), Observed hemispheric asymmetry in global sea ice changes, *Science*, *278*(5340), 1104–1106, doi:10.1126/science.278.5340.1104.

Cherry, S. (1997), Some comments on singular value decomposition analysis, *J. Clim.*, *10*, 1759–1761, doi:10.1175/1520-0442(1997)010<1759:SCOSVD>2.0.CO;2.

Comiso, J. (1999), Bootstrap sea ice concentrations from NIMBUS-7 SMMR and DMSP SSM/I, 26 October 1978 through 31 December 2007, Natl. Snow and Ice Data Cent., Boulder, Colo., updated 2008. (Available at http://nsidc.org/data/docs/daac/nsidc0079_bootstrap_seaice.gd.html)

Comiso, J. C., C. L. Parkinson, R. Gersten, and L. Stock (2008), Accelerated decline in the Arctic sea ice cover, *Geophys. Res. Lett.*, *35*, L01703, doi:10.1029/2007GL031972.

Deser, C., J. E. Walsh, and M. S. Timlin (2000), Arctic sea ice variability in the context of recent atmospheric circulation trends, *J. Clim.*, *13*, 617–633, doi:10.1175/1520-0442(2000)013<0617:ASIVIT>2.0.CO;2.

Deser, C., R. Tomas, M. Alexander, and D. Lawrence (2010), The seasonal atmospheric response to projected Arctic sea ice loss in the late twenty-first century, *J. Clim.*, *23*, 333–351, doi:10.1175/2009JCLI3053.1.

Finnis, J., M. M. Holland, M. C. Serreze, and J. J. Cassano (2007), Response of Northern Hemisphere extratropical cyclone activity and associated precipitation to climate change, as represented by the Community Climate System Model, *J. Geophys. Res.*, *112*, G04S42, doi:10.1029/2006JG000286.

Francis, J. A., W. Chan, D. J. Leathers, J. R. Miller, and D. E. Veron (2009), Winter Northern Hemisphere weather patterns remember summer Arctic sea-ice extent, *Geophys. Res. Lett.*, *36*, L07503, doi:10.1029/2009GL037274.

Gerdes, R. (2006), Atmospheric response to changes in Arctic sea ice thickness, *Geophys. Res. Lett.*, *33*, L18709, doi:10.1029/2006GL027146.

Hassol, S. J. (2004), *Impacts of a Warming Arctic: Arctic Climate Impact Assessment*, 139 pp., Cambridge Univ. Press, Cambridge, U.K.

Holland, M. M., C. M. Bitz, and B. Tremblay (2006), Future abrupt reductions in the summer Arctic sea ice, *Geophys. Res. Lett.*, *33*, L23503, doi:10.1029/2006GL028024.

Honda, M., K. Yamazaki, H. Nakamura, and K. Takeuchi (1999), Dynamic and thermodynamic characteristics of atmospheric response to anomalous sea-ice extent in the Sea of Okhotsk, *J. Clim.*, *12*, 3347–3358, doi:10.1175/1520-0442(1999)012<3347:DATCOA>2.0.CO;2.

Honda, M., J. Inoue, and S. Yamane (2009), Influence of low Arctic sea-ice minima on anomalously cold Eurasian winters, *Geophys. Res. Lett.*, *36*, L08707, doi:10.1029/2008GL037079.

Kvamstø, N. G., P. Skeie, and D. B. Stephenson (2004), Impact of Labrador sea-ice extent on the North Atlantic Oscillation, *Int. J. Climatol.*, *24*, 603–612, doi:10.1002/joc.1015.

Lanzante, J. R. (1984), A rotated eigenanalysis of the correlation between 700 mb heights and sea surface temperatures in the Pacific and Atlantic, *Mon. Weather Rev.*, *112*, 2270–2280, doi:10.1175/1520-0493(1984)112<2270:AREOTC>2.0.CO;2.

Lawrence, D. M., A. G. Slater, R. A. Tomas, M. M. Holland, and C. Deser (2008), Accelerated Arctic land warming and permafrost degradation during rapid sea ice loss, *Geophys. Res. Lett.*, *35*, L11506, doi:10.1029/2008GL033985.

Magnusdottir, G., C. Deser, and R. Saravanan (2004), The effects of North Atlantic SST and sea-ice anomalies on the winter circulation in CCM3: 1. Main features and storm-track characteristics of the response, *J. Clim.*, *17*, 857–876, doi:10.1175/1520-0442(2004)017<0857:TEONAS>2.0.CO;2.

Parkinson, C. L., D. J. Cavalieri, P. Gloersen, H. J. Zwally, and J. C. Comiso (1999), Arctic sea ice extents, areas, and trends, 1978–1996, *J. Geophys. Res.*, *104*(C9), 20,837–20,856, doi:10.1029/1999JC900082.

Prohaska, J. T. (1976), A technique for analyzing the linear relationships between two meteorological fields, *Mon. Weather Rev.*, *104*, 1345–1353, doi:10.1175/1520-0493(1976)104<1345:ATFATL>2.0.CO;2.

Räisänen, J. (2008), Warmer climate: Less or more snow?, *Clim. Dyn.*, *30*(2–3), 307–319, doi:10.1007/s00382-007-0289-y.

Rajagopalan, B., E. Cook, U. Lall, and B. K. Ray (2000), Spatiotemporal variability of ENSO and SST teleconnections to summer drought over the United States during the twentieth century, *J. Clim.*, *13*, 4244–4255, doi:10.1175/1520-0442(2000)013<4244:SVOEAS>2.0.CO;2.

Rothrock, D. A., Y. Yu, and G. A. Maykut (1999), Thinning of the Arctic sea-ice cover, *Geophys. Res. Lett.*, *26*(23), 3469–3472, doi:10.1029/1999GL010863.

Serreze, M. C., and J. A. Francis (2006), The Arctic amplification debate, *Clim. Change*, *76*(3–4), 241–264, doi:10.1007/s10584-005-9017-y.

Serreze, M. C., M. M. Holland, and J. Stroeve (2007), Perspectives on the Arctic's shrinking sea-ice cover, *Science*, *315*, 1533–1536, doi:10.1126/science.1139426.

Serreze, M. C., A. P. Barrett, J. C. Stroeve, D. N. Kindig, and M. M. Holland (2009), The emergence of surface-based Arctic amplification, *Cryosphere*, *3*, 11–19, doi:10.5194/tc-3-11-2009.

Simmonds, I., and K. Keay (2009), Extraordinary September Arctic sea ice reductions and their relationships with storm behavior over 1979–2008, *Geophys. Res. Lett.*, *36*, L19715, doi:10.1029/2009GL039810.

Singarayer, J. S., J. L. Bamber, and P. J. Valdes (2006), Twenty-first-century climate impacts from a declining Arctic sea ice cover, *J. Clim.*, *19*, 1109–1125, doi:10.1175/JCLI3649.1.

Stroeve, J. C., M. C. Serreze, F. Fetterer, T. Arbetter, W. Meier, J. Maslanik, and K. Knowles (2005), Tracking the Arctic's shrinking ice cover: Another extreme September minimum in 2004, *Geophys. Res. Lett.*, *32*, L04501, doi:10.1029/2004GL021810.

Stroeve, J., M. M. Holland, W. Meier, T. Scambos, and M. C. Serreze (2007), Arctic sea ice decline: Faster than forecast, *Geophys. Res. Lett.*, *34*, L09501, doi:10.1029/2007GL029703.

Stroeve, J., A. Frei, J. McCreight, and D. Ghatak (2008), Arctic sea-ice variability revisited, *Ann. Glaciol.*, *48*(1), 71–81, doi:10.3189/172756408784700699.

Wallace, J. M., C. Smith, and C. S. Bretherton (1992), Singular value decomposition of wintertime sea surface temperature and 500-mb height anomalies, *J. Clim.*, *5*, 561–576, doi:10.1175/1520-0442(1992)005<0561:SVDOWS>2.0.CO;2.

Yang, D., D. L. Kane, L. D. Hinzman, X. Zhang, T. Zhang, and H. Ye (2002), Siberian Lena River hydrologic regime and recent change, *J. Geophys. Res.*, *107*(D23), 4694, doi:10.1029/2002JD002542.

Ye, B., D. Yang, and D. L. Kane (2003), Changes in Lena River streamflow hydrology: Human impacts versus natural variations, *Water Resour. Res.*, *39*(7), 1200, doi:10.1029/2003WR001991.

Ye, H., D. Yang, and D. Robinson (2008), Winter rain on snow and its association with air temperature in northern Eurasia, *Hydrol. Process.*, *22*(15), 2728–2736, doi:10.1002/hyp.7094.

A. Frei, Department of Geography, Hunter College, Program in Earth and Environmental Sciences, City University of New York, Graduate Center, 365 Fifth Ave., New York, NY 10016, USA.

D. Ghatak, Program in Earth and Environmental Sciences, CUNY Graduate Center, City University of New York, 365 Fifth Ave., New York, NY 10016, USA. (dghatak@gc.cuny.edu)

G. Gong, Department of Earth and Environmental Engineering, Columbia University, 918 S.W. Mudd Hall, Mail Code 4711, 500 W. 120th St., New York, NY 10027, USA.

D. Robinson, Department of Geography, Rutgers University, Piscataway, NJ, USA.

J. Stroeve, National Snow and Ice Data Center, CIRES, University of Colorado, 449 UCB Boulder, CO 80309-0449, USA.